ELSEVIER

FEMS Microbiology Ecology 53 (2005) 73–87

FEMS MICROBIOLOGY Ecology

www.fems-microbiology.org

Extremotrophs, extremophiles and broadband pigmentation strategies in a high arctic ice shelf ecosystem

Derek R. Mueller [a,*], Warwick F. Vincent [a], Sylvia Bonilla [a,b], Isabelle Laurion [c]

[a] *Centre d'études nordiques et Département de biologie, Université Laval, Pavillon Vachon, Quebec City, QC, Canada G1K 7P4*
[b] *Facultad de Ciencias, Universidad de la República, Montevideo, Uruguay*
[c] *Institut national de la recherche scientifique, Centre Eau, Terre et Environnement, Quebec City QC, Canada*

Received 30 June 2004; received in revised form 5 November 2004; accepted 5 November 2004

First published online 23 November 2004

Abstract

Remnant ice shelves along the northern coast of Ellesmere Island, Nunavut, Canada (~83°N) provide a habitat for cryo-tolerant microbial mat communities. Bioassays of bacterial and primary production were undertaken to quantify the short-term physiological response of the mats to changes in key variables that characterize this cryo-ecosystem (salinity, irradiance and temperature). The heterotrophic versus autotrophic community responses to these stressors differed markedly. The heterotrophic bacteria were extremophilic and specifically adapted to ambient conditions on the ice shelf, whereas the autotrophic community had broader tolerance ranges and optima outside the ambient range. This latter, extremotrophic response may be partly due to a diverse suite of pigments including oligosaccharide mycosporine-like amino acids, scytonemins, carotenoids, phycobiliproteins and chlorophylls that absorb from the near UV-B to red wavelengths. These pigments provide a comprehensive broadband strategy for coping with the multiple stressors of high irradiance, variable salinity and low temperatures in this extreme cryo-environment.

Keywords: Ice shelf; Microbial mats; Scytonemin; Oligosaccharide mycosporine-like amino acid; Productivity; Extremophile; Extremotroph

1. Introduction

Microbial phototrophs occur in a wide range of ice-bound environments including sea ice, glaciers and snow [1]. More recently, another type of cryo-ecosystem has been discovered in the North Polar Region. Similar to their Southern Hemisphere equivalents, arctic ice shelves provide an extreme habitat for microbiota. Microbial mats constitute the dominant biomass on the Ward Hunt Ice Shelf, High Arctic Canada (latitude 83°04′N, longitude 74°25′W). These are a complex microbial consortia dominated by cyanobacteria (notably the genera *Phormidium*, *Leptolyngbya*, *Nostoc* and *Gloeocapsa*) but also containing a wide variety of other taxa including viruses, heterotrophic bacteria, green micro-algae and diatoms, as well as micro-invertebrates [2,3].

Polar microbial mat communities retain a large overwintering biomass and then grow slowly during the brief season of liquid water availability [4]. The micro-organisms on the Ward Hunt Ice Shelf deal with a combination of physiological stresses imposed by their ambient environment, including cold temperatures (<5 °C), high levels of solar radiation (including ultraviolet radiation) and 10-fold variations in salinity. The conjunction of these conditions makes arctic ice shelves an extreme habitat type, however the physiological optima and tolerance ranges of 'ice-mat' communities in relation to these stressors have not been quantified.

* Corresponding author. Tel.: +418 656 2131x8153; fax: +418 656 2043.
E-mail address: derek.mueller@bio.ulaval.ca (D.R. Mueller).

0168-6496/$22.00
doi:10.1016/j.femsec.2004.11.001

Many polar microbial mat cyanobacteria are cold-tolerant (psychrotrophic) rather than cold-adapted (psychrophilic) with their thermal optima for photosynthesis and growth lying well above their ambient range [5,6]. By extension, polar phototrophs may respond to several aspects of their habitats in the same way, with tolerance to extremes in various environmental dimensions (extremotrophs) rather than adaptation towards optimal growth at or near the extreme conditions experienced in situ (extremophiles). Microbial mats elsewhere are known to reduce the effects of high ultraviolet (UV) radiation with photo-protectants that quench free radicals or act as screening pigments [7,8]. Polar microbial mats are simultaneously exposed to high UV irradiances, high photosynthetically active radiation (PAR) and low temperatures, leaving them particularly prone to photodamage [9], and suggesting that photoprotection may be especially important in these systems. In this multi-stressor environment, a broadband pigment strategy that efficiently reduces photodamage might also free up resources for osmoregulation, thereby assisting in salinity, freeze–thaw and desiccation tolerance, and preventing serious damage when these other stressors inhibit metabolic activity and cellular repair mechanisms.

The purpose of this paper is to evaluate the physiological attributes of mats in the Ward Hunt Ice Shelf cryo-ecosystem and to address the question of how these consortia respond to physical and chemical stresses in their high arctic environment. These communities occur today in the Arctic and Antarctica, but may have been more widespread during periods of extreme cooling in the past [10]. We first quantified the primary production and bacterial heterotrophic production of northern ice shelf microbial mat consortia under representative mid-melt season conditions. We then addressed the hypothesis that these mats subsist in sub-optimal conditions by determining their metabolic response to short-term changes in light regime, temperature, salinity and hydration. We identified and quantified pigments (including UV absorbing compounds, some of which may be transparent in the PAR waveband) in these microbial mats, specifically chlorophylls, carotenoids, scytonemins and mycosporine-like amino acids (MAAs), to determine to what extent the potential for photoprotection exists within these communities.

2. Methods

2.1. Study site

The Ward Hunt Ice Shelf is a ~40 m thick free-floating mass of ice that accreted in situ over the last 4500 years [11]. The surface of the ice shelf is marked by a ridge and trough morphology that is associated with meltwater lakes (up to 15 km long, ~3 m deep and 10–20 m wide), which run parallel to the Ellesmere Island coastline (Fig. 1).

The distribution of microbial mats across the ice shelf is highly variable. Typically, microbial mats occur in conjunction with sparse sediment deposits either on the ice surface or in discrete depressions in the ice surface termed cryoconite holes (approximately 7% cover; D.R. Mueller, unpublished data). In certain areas, where sediment has been concentrated over time [12] microbial mats appear to be more developed and are relatively abundant (18–31% cover over scales of hundreds of metres; D.R. Mueller, unpublished data).

Arctic ice shelf microbial mats are typically composed of small olive-green flakes or 'matlets' that accumulate to a thickness of several millimetres to centimetres. In more developed communities, the surface layer (100–500 μm) is a conspicuous orange colour [3]. Aside from a surface layer, seen in developed communities and a black, anoxic layer, observed in very thick sediments, these microbial mats do not appear to be further stratified as found in many microbial mats [13].

Microbial mats from northern ice shelves are subjected to a variety of environmental stressors. Furthermore, these stressors vary both temporally and spatially, necessitating physiological acclimation on several timescales. A pronounced seasonality at this high latitude site causes gradual but extreme changes in light photoperiod (147 days of continuous darkness in winter and 147 days of continuous light in summer) and irradiance (0–1200 μmol photons m^{-2} s^{-1} downwelling PAR), temperature (average mat temperature = −8.6 °C, maximum = 1.7 °C, minimum = −15.7 °C; D.R. Mueller, unpublished data from automated in situ dataloggers) and the availability of liquid water.

During the summer months, the ice shelf environment is more dynamic due to temperature shifts across the freezing point of water. Microbial mats emerge sporadically from under melting snow and ice over the course of the summer months resulting in a ~10-fold increase in light levels. Periods of high irradiances due to low so-

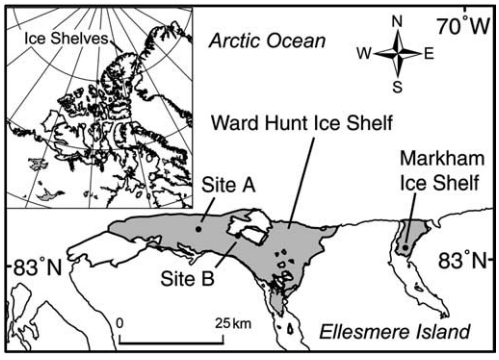

Fig. 1. Location of ice shelves in Nunavut, Canada.

lar angles and reflection from high albedo surfaces such as snow and ice are punctuated by periods of intense fog in which ambient irradiances are much reduced. In spring, meltwater influx reduces the salinity of water that overlies the microbial mats, with conductivities ranging from fresh (0.5 mS cm^{-1}) during periods of open water to saline (>10 mS cm^{-1}) during freeze-up. During summer, in the absence of turbulent mixing, density stratified waters near to the microbial mat surface can be 4–10 times more saline than surface waters [3]. Summer air temperatures rarely exceed 10 °C over the Ward Hunt Ice Shelf and the temperature of the water that immerses microbial mats does not rise higher than a few degrees, yet the temperature of microbial mats that are not overlain by water can exceed 5 °C (D.R. Mueller, unpublished data). Environmental variables change on timescales from minutes to seasons, yet many of these changes are event-driven and occur on relatively short timescales (minutes to hours). Therefore our short-term acclimation experiments capture some but not all of the possible acclimation scenarios for ice shelf micro-organisms. While a short-term acclimation response will not elucidate the full tolerance range of these micro-organisms, it will serve as a proxy indicator to determine if physiological optima occur within the range of conditions that are prevalent in their cryo-habitat.

2.2. Primary productivity assays

Microbial mats from the Ward Hunt Ice Shelf were collected in August of 2002 and July 2003, with sampling focussed on the thickest, most developed communities. Mats were placed in plastic trays, covered and returned to a nearby field laboratory, where they were prepared for assay.

Microbial mats were cored at random using a 1 cc syringe (area = 0.2 cm^2) with the tip removed. Five replicates per treatment were placed in separate Whirl–Paks (Nasco, Fort Atkinson, WI), which contained 20 ml of ice shelf surface meltwater, spiked with ^{14}C labelled $NaHCO_3$ yielding a final activity of 0.6 μCi ml^{-1}. Each core of microbial mat partially disintegrated in the incubation water due to a lack of mat cohesion, so the observed rates may represent an overestimate relative to mats in which diffusion limitation is more severe, such as intact cohesive mats. The dissolved inorganic carbon (DIC) concentration of the incubation water was determined by acidification and infrared gas analysis (IRGA) by the National Laboratory for Environmental Testing, Burlington, Ontario.

Whirl–Paks were sealed, gently mixed and placed in plastic neutral density filter envelopes. The absorption spectra of the filters and Whirl–Paks were determined using a Hewlett–Packard 8452A diode-array spectrophotometer (Palo Alto, CA) equipped with an integrating sphere. The filters did not affect the spectral distribution of light between 400 and 700 nm. The treatments reduced PAR levels to 0 (dark), 1%, 6%, 10% and 22%, 45% and 82% of ambient light. UV-A (320–400 nm) levels were 5%, 8%, 11%, 17%, 35% and 80% of ambient and UV-B (300–320 nm, in this case) levels were 26%, 28%, 34%, 36%, 42% and 85% of ambient light. Samples were placed outside on snow or in white Styrofoam incubators for a period of 4–5 h. Downwelling and scalar PAR irradiances were monitored at regular intervals throughout the experiment using a Licor 190SA quantum sensor (Licor Biosciences, Lincoln, NE), a QSL100 quantum scalar sensor (Biospherical Instruments, San Diego, CA) and a LI 1440 datalogger (Licor Biosciences, Lincoln, NE). The microbial mat samples were exposed to light from all directions and therefore, 4π irradiance was used for further calculations and when the 4π irradiance was not available (2002), it was estimated from 2π irradiance using the empirical relationship ($4\pi = 3.6(2\pi)$, $R^2 = 0.66$, $n = 293$), determined in 2003. Temperature was measured inside the incubators by using Stowaway temperature loggers (Onset Computer Corporation, Bourne, MA). The incubations were stopped by filtering microbial mats onto GC50 glass-fibre filters (AMD Manufacturing, Mississauga) and acidification with 200 μl of 0.1 N HCl. Filters were stored frozen until analysis.

In the laboratory, filters were placed in scintillation vials and further acidified by fumigation for 24 h. Liquid scintillation cocktail (Beckman Ready Safe, Fulerton, CA and OptiPhase 'HiSafe' 2, Perkin–Elmer, Boston, MA) was added and samples were homogenized using glass rods prior to determination of specific activity on a Beckman LS 6500 scintillation counter (Fulerton, CA). Treatments were corrected for β-carboxylation by subtracting dark ^{14}C uptake [14] and data were fitted to the hyperbolic equation of Platt et al. [15] using an iterative non-linear approach (Sigma Plot 8.0, Systat Software, Point Richmond, CA). Values for the light saturation index (E_k) were calculated from the relationship $E_k = P_{max}/\alpha$. P_{max} was calculated by using the method outlined by Platt et al. [15].

2.3. Bacterial productivity assays

Heterotrophic bacterial productivity was determined by tritiated leucine uptake [16]. Samples were prepared as above with a leucine concentration of 10 nM and an activity of 0.5 μCi ml^{-1}. Incubations were carried out on five replicates in darkness and were terminated with the addition of trichloroacetic acid (TCA) to a final concentration of 5% (v/v) followed by heating to 80 °C for 15 min and then filtration onto cellulose acetate filters [17]. Filters were rinsed twice with 5% TCA (3 ml) and then twice with 80% ethanol (2 ml), placed in scintillation vials to dry and were frozen for transport [16].

Filters were dissolved with 0.5 ml of ethyl acetate and radioactivity was determined 24 h following the addition of scintillation cocktail and glass rod homogenization. Samples were corrected for leucine adsorption by using the scintillation counts of TCA killed replicates (dead counts were typically 3% of live counts). Bacterial carbon production was then estimated using a conversion factor of 3.1 kg C mol leucine^{-1} and an isotope dilution of two [16].

2.4. Temperature effects

Microbial mat primary and bacterial production were assayed at 0, 5, 10, 15 and 20 °C, using the methodology outlined above. Water baths were prepared at the correct temperatures and microbial mat samples (acclimated to ~4 °C) were immersed in the water baths in their hermetically sealed Whirl–Paks, while the temperature was constantly monitored for the incubation period using a hand-held temperature probe (Digithermo 4550, IMEC GmbH, Heilbronn Germany). Additional temperature measurements made with 4 Stowaway temperature loggers indicated that conditions inside the filters were actually 2.6, 5.2, 10.4 and 15.3 °C for the first four treatments. For primary productivity, only a dark and 45% filter treatment (average irradiance = 1596 μmol photons m^{-2} s^{-1}) were used (to capture photosynthetic rate in the plateau region of the *P* vs. *E* curve), whereas bacterial productivity was determined with dark live and dead treatments.

2.5. Salinity effects

Mat productivity was determined at 4 different salinities (0.1, 2.9, 10 and 29 mS cm^{-1}), which were obtained by mixing de-ionized water, ice shelf water (0.4 mS cm^{-1}) and locally sampled Arctic Ocean seawater (29 mS cm^{-1}) at the appropriate ratios. Arctic ice shelves are partly derived from sea ice and the ionic composition of ice shelf surface water is consistent with the dilution of seawater [3]. For primary production, dark and 45% PAR treatments were used (average irradiance = 1607 μmol photons m^{-2} s^{-1}), while bacterial production was determined with live and dead treatments. Differences in incubation water DIC between the treatment groups were accounted for in the primary productivity calculations.

2.6. Desiccation effects

Microbial mats were collected in plastic trays and dried in the sun over the course of five days (water content was reduced to 3% (w/w), SE = 0.8%, $n = 3$). Approximately 5 min prior to the experiment, the dried mats were re-wet using ice shelf water and were incubated along with fresh, moist mats (water content = 48% (w/w), SE = 1.6%, $n = 3$) according to the methodology above. Primary productivity was measured with the five filters, full PAR and dark treatments and bacterial productivity was determined with live and dead treatments.

2.7. Light transition effects

Microbial mats were collected from two contrasting micro-habitats on the ice shelf. The first micro-site was exposed to full sunlight whereas the second micro-site contained microbial mats that were shaded from direct sunlight by a ~20 cm cover of snow. The latter micro-site had irradiances of approximately 10% of ambient PAR due to the overlying snow cover. Exposed and shaded mats were returned to the field laboratory in dark containers, but upon arrival they were placed either on top of snow or buried under snow to simulate the two micro-sites on the ice shelf. There were two light transitions: (1) exposed to shaded; (2) shaded to exposed to simulate changes in light levels during melt-out and freeze-up, respectively. These experimental groups were accompanied by control groups: (1) exposed to exposed; (2) shaded to shaded. After an 18-h acclimation period, cores of these mats were incubated for primary productivity (*P* vs. *E*) determination using the methodology described above. For the exposed to shaded group, treatments 1%, 6%, 11% and 22% had 3 replicates, 45% had 1 replicate and the 82% treatment was not performed due to the lack of radiolabel.

2.8. Biomass and chlorophyll a determination for productivity

Microbial mats were sampled for chlorophyll *a* determination using a 0.64 cm^2 core. These samples were stored frozen and in the dark for transport. In the laboratory, samples were thawed in 6 ml 90% acetone:water (v/v) and sonicated (Microson XL2000, Misonix, Farmingdale, NY) at approximately 10 W for two 30-s bursts with a pause of 30 seconds between sonication steps. Pigment extraction took place in the dark for 1 h at 4 °C and terminated with centrifugation at 4000 rpm for 5 min at 4 °C. The supernatant was removed and chlorophyll *a* concentrations were determined at 663 and 750 nm, before and after acidification, in a Cary 300 Bio UV–Vis spectrophotometer (Varian, Mulgrave, Australia) [18]. This procedure was carried out three times to ensure complete extraction and total chlorophyll *a* content was determined by summing each extraction [19]. Microbial mat free water content and biomass were determined from 4.15 cm^2 cores that were collected and frozen for transport. In the laboratory, the cores were weighed and then dried to constant weight at 100 °C. The mass of organic and inorganic fractions were determined by loss on ignition at 500 °C for seven hours.

2.9. HPLC pigment structure determination

For determination of pigment structure three ice shelf sites were visited on the northern Ellesmere Island coastline (Fig. 1): Ward Hunt Ice Shelf Site A (83°05.6′N, 75°08.0′W), Ward Hunt Ice Shelf Site B (83°05.0′N, 74°25.3′W) and Markham Ice Shelf (83°02.4′N, 71°26.5′W). Site A was characterized by sparse sediment in cryoconite holes, whereas the other two sites had thick microbial mats with orange surface layers. Site B mats were also used in the productivity assays. At each main site, 7 replicate cores (0.64 cm^2) were taken from micro-sites in the immediate vicinity. Cores were frozen, transported to Quebec and transferred into −80 °C storage until analysis by reverse-phase high performance liquid chromatography (HPLC).

Microbial mat cores were thawed, ground with a Caframo R2R1 tissue grinder (Wiarton, Ontario) and sonicated as described above in 5 ml 90% acetone:water (v/v). Pigments were left to extract under argon at −20 °C for 20 h and then centrifuged. The supernatant was filtered on a 0.2 μm pore size PTFE Acrodisc filter (Pall Corporation, Ann Arbor, MI) and 50 μl of the sample was injected into a Varian ProStar HPLC (Mulgrave, Australia) at a flow rate of 1 ml min^{-1}. The mobile phase was a gradient of two eluents, methanol:acetonitrile:aqueous pyridine solution (50:25:25, v/v/v) and methanol:acetonitrile:acetone (20:60:20, v/v/v) [20]. The stationary phase consisted of a Symmetry C_8 column (3.5 μm pore size, 4.6 × 150 mm) at 25 °C with a Symmetry C_8 guard column (5 μm pore size, 3.9 × 20 mm) (Waters Corporation, Milford, MA). Pigments were detected and quantified using two photodiode array channels (450 nm for carotenoids and 384 nm for scytonemins) and a fluorescence channel (excitation at 440 nm and emission at 650 nm) for chlorophylls. Pigments were identified by retention time and verified by absorption spectra (350–750 nm), for all pigments except chlorophyll *c2*, pheophorbide-like and a chlorophyll *b*-related peak, which were identified by retention time only. Purchased standards (chlorophyll *a*, chlorophyll *b*, chlorophyll *c2*, β-carotene, echinenone, canthaxanthin, lutein, zeaxanthin, violaxanthin, diadinoxanthin, myxoxanthophyll and fucoxanthin) were used to convert peak areas to pigment concentrations for these compounds and related chlorophylls. Other carotenoids were quantified by using peak areas in conjunction with published extinction coefficients of closely related pigments (4-keto-myxol-2′-methylpentoside-like, 125.3 l g^{-1} cm^{-1}; myxoxanthophyll-related, 125.3 l g^{-1} cm^{-1}; canthaxanthin-related, 207.5 l g^{-1} cm^{-1}), spectrally modified extinction coefficients (oscillaxanthin, 54 l g^{-1} cm^{-1} at 450 nm from 75 l g^{-1} cm^{-1} at 490 nm [21]), or the extinction coefficient of β-carotene (250 l g^{-1} cm^{-1}) for unknown carotenoids [22]. Scytonemin and related pigments were quantified with an extinction coefficient of 112.6 l g^{-1} cm^{-1} at 384 nm [23].

2.10. MAA determination

Mycosporine-like amino acids were separated, identified and quantified by reverse-phase isocratic HPLC [24]. Microbial mat cores were sampled, ground and sonicated as described in the previous section, but were extracted using 5 ml 25% aqueous methanol (v/v) at 45 °C for 2 h [25]. Extracts were centrifuged, filtered with 0.2 μm nylon Acrodisc filters (Pall Corporation, Ann Arbor, MI) and stored under argon prior to HPLC analysis. A 50 μl aliquot of sample was injected into the HPLC at a flow rate of 0.5 ml min^{-1}. The mobile phase was 25% aqueous methanol (v/v) with 0.1% acetic acid (v/v) and the stationary phase consisted of a Phenosphere C_8 column (5 μm pore size, 4.6 × 250 mm) (Phenomenex, Torrance, CA) at 26 °C preceded by a Brownlee RP-8 Spheri-5 guard column (4.6 × 30 mm) (Perkin–Elmer, Shelton, CT). MAA compounds were detected and quantified using 5 photodiode array channels (310, 320, 330, 334 and 360 nm). Oligosaccharide mycosporine-like amino acids (OS-MAA) peak areas at 310 nm were converted to concentration units by using the extinction coefficient 17 l g^{-1} cm^{-1} [26]. This group of compounds is heterogeneous and not fully separable from each other using standard MAA methods, a problem that may have been aggravated by our choice of column (which showed poor separability with MAA secondary standards). Therefore, absolute quantities of OS-MAA should be interpreted with caution [26].

3. Results

3.1. Primary and bacterial productivity

The ice shelf microbial mat had a maximum photosynthetic rate (P_{max} for non-treatment groups) ranging from 0.059 to 0.17 g C g Chl a^{-1} h^{-1} (mean = 0.10, SE = 0.025, n = 5) on a per unit chlorophyll *a* basis giving production rates on a per area basis of 27.3–105 mg C m^{-2} h^{-1} (mean = 63.7, SE = 15.2, n = 5) (Table 1). The bacterial productivity was three orders of magnitude lower than primary productivity, ranging from 0.085 to 0.38 μg C g biomass^{-1} h^{-1} (mean = 0.23, SE = 0.15, n = 2) yielding 0.037–0.21 mg C m^{-2} h^{-1} (mean = 0.12, SE = 0.087, n = 2), on a per area basis. The relative contribution of these processes reflects the overwhelming dominance of autotrophic biomass relative to heterotrophic bacteria in the mats. Photosynthesis versus irradiance models revealed very small α values,

Table 1
Microbial mat primary and bacterial productivity parameters under different experimental conditions

Treatment	Productivity parameter							
	P_s	α	β	P^1_{max}	P^2_{max}	E_k	BP[1]	BP[2]
T_0 conditions								
Low light	0.105* (0.021)	0.0005* (0.00004)	0.0001* (0.00005)	0.059	27.3	106	–	–
High light	0.057 (0.102)	0.0001* (0.00004)	<0.000001 (0.00007)	0.057	54.8	566	0.085 (0.007)	0.037 (0.003)
Light transition 1								
Exposed to shaded	0.17 (0.078)	0.0054* (0.0011)	0.0004 (0.0007)	0.13	80.4	24.2	–	–
Shaded to shaded (control)	0.20* (0.038)	0.007* (0.0012)	0.0003 (0.0003)	0.17	105.2	24.2	–	–
Light transition 2								
Shaded to exposed	0.22* (0.011)	0.0005* (0.00001)	<0.00004* (0.000007)	0.17	105.2	332	–	–
Exposed to exposed (control)	0.15* (0.031)	0.0004* (0.0001)	<0.000001 (<0.00001)	0.15	92.8	367	–	–
Desiccation/rewetting								
Dry to wet							0.038 (0.007)	0.021 (0.004)
Wet to wet (control)	0.064* (0.021)	0.00015* (0.00003)	<0.000001 (0.000009)	0.06	38.7	432	0.384 (0.016)	0.212 (0.009)

P_s is the light-saturated maximum photosynthesis in the absence of photoinhibition (g C g Chl a^{-1} h^{-1}), α is the maximum light utilization coefficient (g C g Chl a^{-1} h^{-1} (μmol photons m^{-2} s^{-1})$^{-1}$), β is the photoinhibition parameter (g C g Chl a^{-1} h^{-1} (μmol photons m^{-2} s^{-1})$^{-1}$), P^1_{max} is the maximum photosynthetic rate per unit Chlorophyll *a* (g C g Chl a^{-1} h^{-1}), P^2_{max} is the maximum photosynthetic rate per unit area (mg C g m^{-2} h^{-1}), E_k is the light saturation index (μmol photons m^{-2} s^{-1}). BP[1] is the bacterial productivity, determined from tritiated leucine uptake per unit biomass (μg C g biomass^{-1} h^{-1}) and BP[2] is the bacterial productivity per unit area (mg C m^{-2} h^{-1}). Standard errors are in parentheses.

* Significant parameter (α = 0.05).

(Table 1) while photoinhibition was minor, with one exception (Fig. 2(a)), suggesting that excess light did not cause considerable damage to the photosynthetic mechanism.

3.2. Effects of temperature

The primary productivity of microbial mats increased monotonically with increasing temperature, suggesting

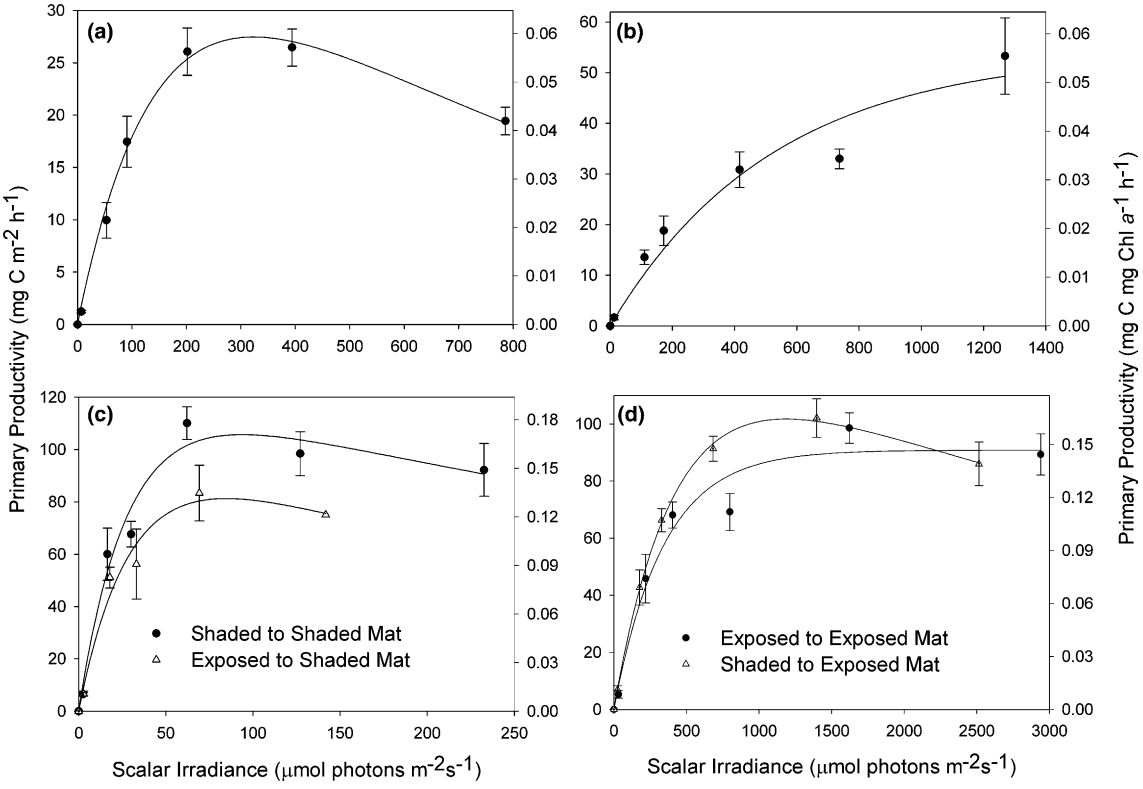

Fig. 2. Photosynthesis versus irradiance for Ward Hunt Ice Shelf microbial mats. Low light conditions (a) were caused by intense fog (August 8, 2002), whereas high light conditions (b) refer to clear sky conditions (July 18, 2003). High scalar irradiances are due to reflection from the white Styrofoam incubators (2003) or snow (2002). (c) Mat acclimatization to high irradiance (shaded to exposed) versus control (exposed to exposed). (d) Mat acclimatization to low irradiance (exposed to shaded) versus control (shaded to shaded).

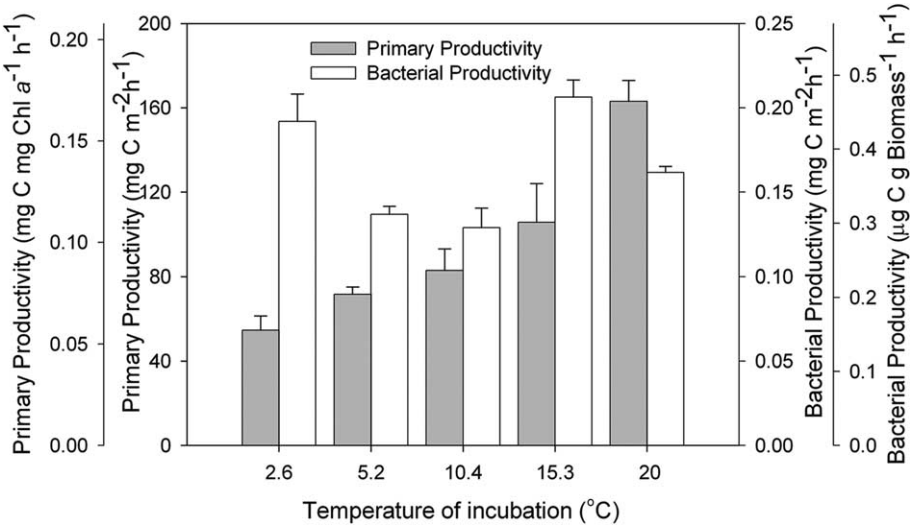

Fig. 3. Effect of temperature on microbial mat productivity on the Ward Hunt Ice Shelf. The primary productivity was measured at ~45% ambient PAR (1596 μmol photons m^{-2} s^{-1}) to avoid potential artifacts due to photoinhibition.

that the physiological tolerance limits lay at temperatures >20 °C, more than 15 °C above maximum ambient temperatures we have recorded in this environment. The treatment at 10.4 °C showed a rate twice that of the normal or ambient (0–5 °C) microbial mat conditions (Fig. 3). In contrast, no coherent relationship was found between bacterial productivity and temperature, with maximum rates at 2.6 and 15.3 °C (Fig. 3).

3.3. Effects of salinity

Primary productivity tripled between the lower salinity treatments and 10 mS cm^{-1} and then returned to a minimum photosynthetic rate at 29 mS cm^{-1} (Fig. 4). Bacterial productivity was maximal at the lowest salinity and dropped by more than 50% over the salinity range (Fig. 4). This suggests that the phototrophic community had a broader salinity optimum range, with peak productivity at higher salinities than mid-season conditions, while the heterotrophic bacterial community appeared to be closely adapted to ambient salinities and poorly adapted to fluctuations relative to the phototrophs.

3.4. Effects of desiccation

Microbial mat desiccation and re-hydration produced inconclusive results for primary productivity with the experimental group departing from the general *P* vs. *E* model response; this precluded the estimation of photosynthetic parameters (Table 1). However, the general trend of both the control and treatment response suggested that there is no apparent effect of desiccation

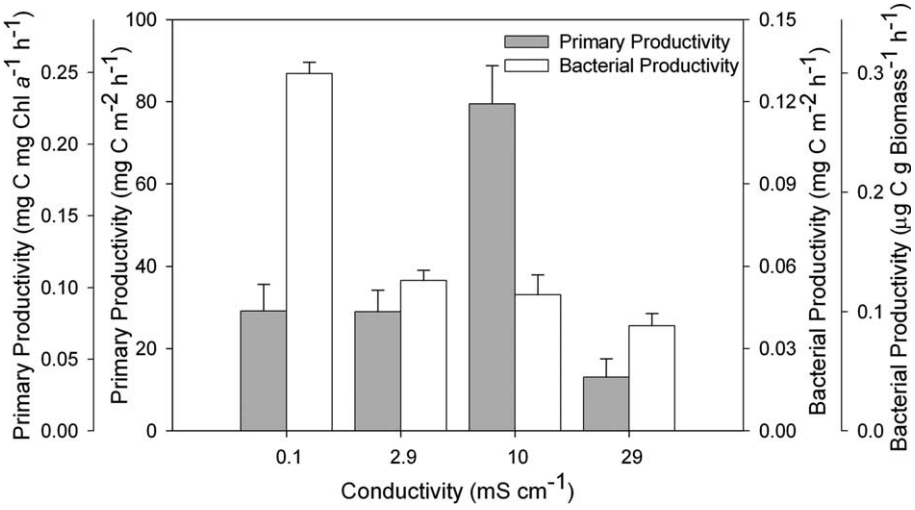

Fig. 4. Effect of conductivity on microbial mat productivity on the Ward Hunt Ice Shelf. The primary productivity was measured at ~45% ambient PAR (1607 μmol photons m^{-2} s^{-1}) to avoid potential artifacts due to photoinhibition.

(not shown). After drying and re-hydration, the bacterial productivity showed a 10-fold significant decrease ($t = -19.8$, $p < 0.001$, $n = 5$) versus the control (Table 1) suggesting that the heterotrophic community was adversely affected by desiccation.

3.5. Effects of light transition

The light acclimation experiment showed only minor differences between control and experimental groups. This suggests that the microbial mats acclimated quickly and effectively to the new light regime that they were assayed under. Some differences include a slightly lower P_{max} for the exposed to shaded transition relative to the shaded to shaded control group (Fig. 2(c)), and a slightly higher P_{max} and β for the shaded to exposed transition relative to the exposed to exposed control group (Fig. 2(d)). Despite this, the P_{max} values for all four groups in the light transition experiments were very close.

3.6. Microbial mat pigments

A diverse assemblage of pigments was identified and quantified from the ice shelf microbial mats (Table 2 and Fig. 5). These include chlorophylls, such as chlorophyll *a*, *b* and *c2*, plus various degradation products (pheophorbide-like, chlorophyllide-like and pheophytin-like

Table 2
Ice shelf microbial mat pigments, mycosporine-like amino acids and ratios of pigments

Pigment/ratio	Ward Hunt Ice Shelf A		Ward Hunt Ice Shelf B		Markham Ice Shelf	
	Concentration (μg cm^{-2}) or ratio (μg μ g^{-1})	SE	Concentration (μg cm^{-2}) or ratio (μg μg^{-1})	SE	Concentration (μg cm^{-2}) or ratio (μg μ g^{-1})	SE
Scytonemin	6.26	1.16	90.47	34.71	6.90	6.05
Red scytonemin	1.66	0.31	137.13	38.37	133.31	39.40
Scytonemin-related	nd	–	2.58	1.66	nd	–
Total scytonemins	**7.92**	1.29	**227.6**	49.06	**140.21**	38.99
Fucoxanthin	0.19	0.19	2.08	0.91	0.31	0.31
Oscillaxanthin-like	0.20	0.20	2.35	0.61	0.59	0.45
Violaxanthin-like	nd	–	nd	–	0.35	0.23
4-keto-myxol-2′-methylpentoside-like	nd	–	3.64	0.88	nd	–
Diadinoxanthin	nd	–	nd	–	1.79	0.76
Myxoxanthophyll	nd	–	7.13	1.24	0.22	0.22
Myxoxanthophyll-related	nd	–	1.13	0.21	0.29	0.14
Zeaxanthin	nd	–	0.79	0.12	0.71	0.07
Lutein	1.24	0.37	2.03	0.27	4.86	0.61
Canthaxanthin-related	nd	–	0.50	0.12	0.11	0.03
Canthaxanthin	0.03	0.03	2.56	0.33	0.47	0.12
Echinenone	0.56	0.15	5.95	0.85	1.58	0.22
β-carotene	0.15	0.04	1.88	0.37	0.98	0.13
Unknown carotenoids	nd	–	2.48	0.70	0.39	0.18
Total carotenoids	**2.36**	0.66	**32.50**	5.26	**12.66**	1.47
Chlorophyll *a*	5.63	0.79	30.58	4.71	17.54	0.96
Chlorophyll *b*	0.80	0.24	1.11	0.13	4.83	0.75
Chlorophyll *c2*	0.29	0.07	0.33	0.10	0.40	0.12
Chlorophyll *a* related 1	0.32	0.07	1.47	0.17	0.67	0.10
Chlorophyll *a* related 2	0.82	0.35	0.16	0.06	0.36	0.11
Chlorophyll *b* related	0.14	0.05	0.28	0.04	0.19	0.04
Chlorophyllide *a*-like	0.41	0.16	0.94	0.35	0.70	0.07
Pheophytin *a*-like	0.14	0.06	0.11	0.04	0.29	0.08
Pheophorbide-like	nd	–	0.57	0.19	0.19	0.08
Unknown chlorophyll	nd	–	0.05	0.03	nd	–
Total chlorophylls	**8.55**	1.48	**35.60**	5.36	**25.16**	1.92
Total MAAs	**13.1**	2.79	**62.6**	16.19	**16.6**	6.03
Scytonemin/chlorophyll *a*	1.49	0.61	4.39	2.22	0.38	0.33
Red scytonemin/chlorophyll *a*	0.35	0.08	4.52	1.39	7.22	1.88
Carotenoids/chlorophyll *a*	0.37	0.07	1.07	0.10	0.72	0.08
OS-MAA/chlorophyll *a*	3.34	1.52	2.35	0.74	1.00	0.38
Scytonemins/carotenoids	19.18	16.13	8.13	2.35	10.65	2.42
OS-MAA/scytonemin	1.93	0.44	0.28	0.04	0.26	0.14
Scytonemin/red scytonemin	3.21	0.93	1.42	0.90	0.09	0.06

Ward Hunt Site A was a blue ice area, whereas the Ward Hunt Site B and Markham Ice Shelf Site were sediment rich areas. Data are an average of seven samples and totals for each category of compounds are in bold. SE indicates standard error and nd signifies not detected.

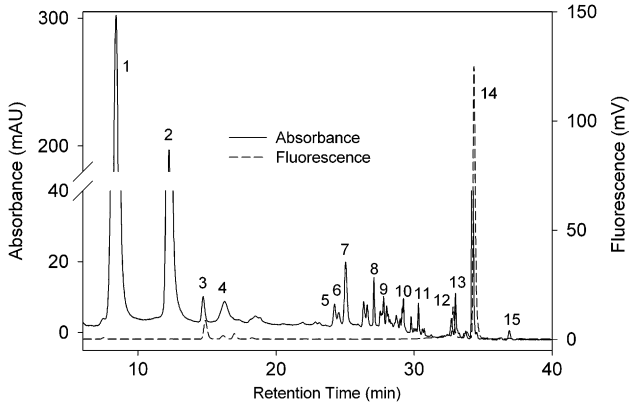

Fig. 5. HPLC chromatogram of microbial mat pigments showing an absorbance channel (440 nm) and a fluorescence channel (excitation 440 nm, emission 650 nm). Peaks are as follows: (1) red scytonemin, (2) scytonemin, (3) chlorophyllide-*a*-like, (4) scytonemin-related, (5) fucoxanthin, (6) oscillaxanthin-like, (7) 4-keto-myxol-2′-methylpentoside-like, (8) myxoxanthophyll, (9) unknown carotenoid (possibly okenone), (10) lutein (left shoulder) and zeaxanthin (main peak), (11) canthaxanthin, (12) chlorophyll *b*, (13) echinenone, (14) chlorophyll *a*, (15) β-carotene. Sample taken from Ward Hunt Ice Shelf Site B.

pigments). Cyanobacterial carotenoids such as echinenone, canthaxanthin (Fig. 6(c)), oscillaxanthin, myxoxanthophyll and a related pigment, the 4-keto-myxol-2′-methylpentoside-like carotenoid (Fig. 6(b)) [27–29] were separated. There were also carotenoids indicating the presence of other taxonomic groups such as chlorophytes (violaxanthin-like carotenoid and lutein), diatoms (fucoxanthin and diadinoxanthin) as well as generally occurring carotenoids such as β-carotene [22]. A bacterial carotenoid, tentatively identified as okenone [30], was found in one sample on the Markham Ice Shelf and in all samples at Ward Hunt Ice Shelf Site B (Fig. 6(d)). The pigment scytonemin was found in many of the microbial mat samples and was often accompanied by its reduced form, red scytonemin (Fig. 6(a)). A pigment with a spectrum similar to scytonemin (max absorbance at 384 nm), but with a retention time about 4 min later, was observed in several samples and may represent a more non-polar derivative of scytonemin. All samples of the ice shelf microbial mats fluoresced strongly red under green excitation when examined by epifluorescence microscopy, indicating the dominance of phycobiliprotein-rich cyanobacteria.

3.7. Microbial mat mycosporine-like amino acids

No 'typical' mycosporine-like amino acids (MAAs) were isolated from the ice shelf microbial mats, such as those found in many species of algae and lower animals [31]. However, there was an abundance of a class of compounds that resembled oligosaccharide MAAs (OS-MAA). These compounds are composed of two chromophores (mycosporine-glycine and likely another MAA) that are linked into a saccharide chain [26]. No

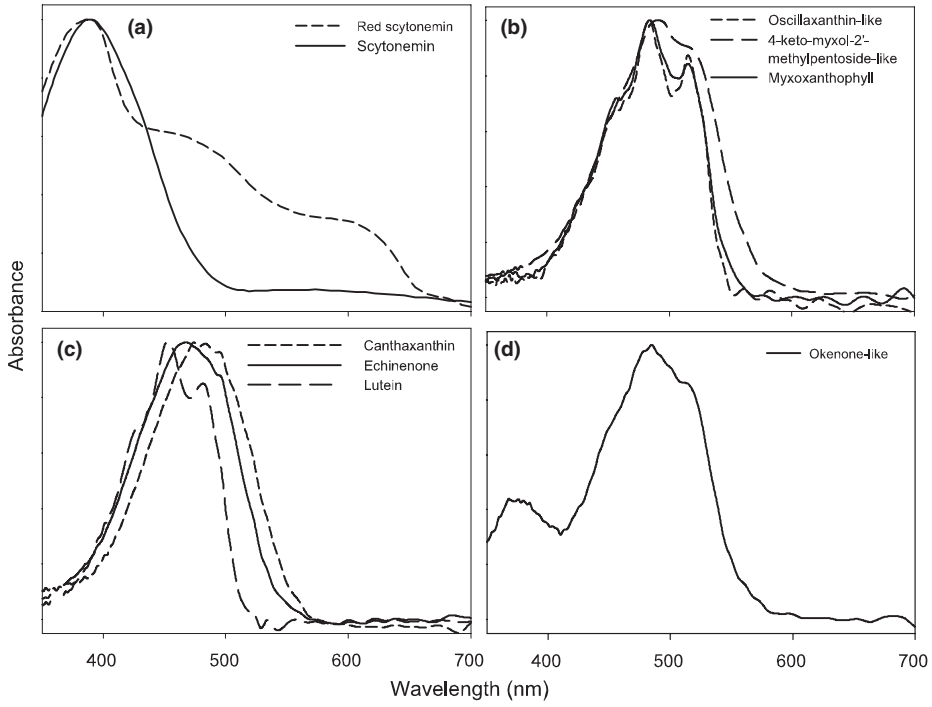

Fig. 6. Spectra of pigments found in arctic ice shelf microbial mats. (a) The UV-A screening cyanobacterial sheath pigment scytonemin and its reduced form, red scytonemin. (b) Cyanobacterial glycosides oscillaxanthin, myxoxanthophyll and a related pigment tentatively identified as 4-keto-myxol-2′-methylpentoside. (c) Carotenoids lutein, canthaxanthin and echinone commonly found in the microbial mats. (d) A bacterial carotenoid tentatively identified as okenone.

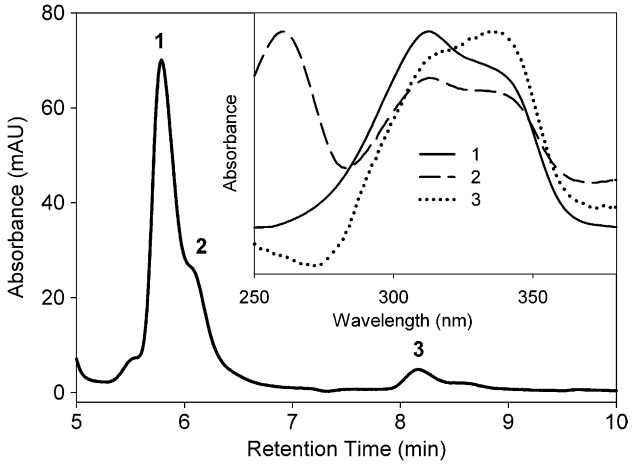

Fig. 7. HPLC chromatogram of microbial mat oligosaccharide mycosporine-like amino acids showing the absorbance at 310 nm. The inset shows the spectra of typical MAA fractions. Peaks are: (1) the primary OS-MAA fraction; (2) an OS-MAA fraction with varying absorbance at 268 nm; (3) an OS-MAA whose 312 and 335 nm chromophores were found to be in different proportions relative to the previous peaks.

method yet exists to separate these compounds completely, and therefore they are treated as a mixture, both here and in the literature [32,33]. The predominant spectral signature of the OS-MAA (peak at 312 and a shoulder at 335 nm) can be seen in Fig. 7 (inset, spectrum 1). As the HPLC retention time increased, several less polar molecules appeared with different spectra, some with differing proportions of the MAA chromophores (Fig. 7, inset, spectrum 3) and others having a secondary peak between 265 and 280 nm (Fig. 7, inset, spectrum 2). This secondary peak may represent a degradation product of the original compound as suggested by others [26,34] or this may be the spectral signature of OS-MAA and water stress proteins as shown by Hill et al. [35].

4. Discussion

4.1. Microbial mat productivity

Many studies of polar microbial mats have been undertaken in Antarctica where conditions are comparable to the Ward Hunt Ice Shelf. In Antarctic ponds, streams and ice shelves cyanobacterial mat gross primary productivity has been measured at rates between 3 and 40 mg C m^{-2} h^{-1} (0.05–0.9 g C g Chl a^{-1} h^{-1}) [36–40]. In the Northern Hemisphere, microbial mats taken from Ward Hunt Lake (adjacent to the Ward Hunt Ice Shelf) had primary productivities of 3.0–6.5 mg C m^{-2} h^{-1} (~0.04 g C g Chl a^{-1} h^{-1})[19]. Our measured primary production rates for the Ward Hunt Ice Shelf mats lie within the range of polar microbial ice mat literature for chlorophyll specific productivity but not for productivity per unit area possibly reflecting the relatively high standing stocks of pigments in these mats. Low chlorophyll *a* specific photosynthetic rates in microbial mats have been attributed to inactive yet intact chlorophyll *a* preserved in senescent cells [40], although this could also be due to self-shading in thick mats.

The maximum light utilization coefficient (α) and the light saturation index (E_k) may be used to assess photoacclimation status when compared to closely analogous systems. Our estimates are similar to those found by Vincent et al. [38] in microbial mats from Antarctic ponds, streams and lakes (0.0003–0.0089 g C g Chl a^{-1} h^{-1} (μmol photons m^{-2} s^{-1})$^{-1}$). Levels of E_k varied substantially and, except for the shaded experiment, greatly exceeded those found by Vincent et al. [38] suggesting high light acclimated physiology. Photoinhibition exhibited in our study may be due to loss of microbial mat integrity and our method of placing mats in water above a highly reflective surface (snow and Styrofoam), which likely increased irradiance to levels beyond what the microbial mats may naturally receive.

Despite the ubiquitous presence of heterotrophic bacteria in microbial mat consortia, bacterial productivity is rarely measured [41]. Bacterial productivity as measured by thymidine uptake in Antarctic microbial mats was found to be 0.2–0.45 pmol thymidine cm^{-2} h^{-1} [40]. Using empirical conversion factors of 2.0×10^{18} cells mol thymidine^{-1} and 10 fg C cell^{-1} [42] a productivity of 0.04–0.09 mg C m^2 h^1 can be estimated. This rate is quite close to the results from the present study. Further methodological improvements such as determination of substrate saturation [43], isotope dilution [16] and conversion factor determination [44] are necessary to ensure complete inter-comparability between ecosystems. Given the potential for high concentrations of leucine within the arctic ice shelf microbial mat environment, the use of generic isotope dilution factors, developed for bacterioplankton, may underestimate productivity substantially.

A first-order estimate of the annual production of this community can be made from the measurements reported here. The standing stock of microbial mat biomass on the Ward Hunt Ice Shelf attains levels of 464 g m^{-2} (SE = 38, $n = 26$). Assuming a representative microbial mat primary productivity of 64 mg C m^{-2} h^{-1} (from mean P_{max} for non-treatment groups, SE = 15, $n = 5$), a growing season of 70 days (D.R. Mueller, unpublished data) and ignoring any potential diel or seasonal effects, the annual gross photosynthesis is approximately 108 g C m^{-2}. With a carbon to biomass ratio of 0.5, the time required to accumulate present standing stocks would be just over 2 years. Respiration rates in microbial mats typically exceed half of the gross photosynthetic rate [45] and would extend the accumulation time estimate by at least a further 2 years. During

this period, bacterial heterotrophy (mean productivity = 0.1 mg C m^{-2} h^{-1}, SE = 0.09 $n = 2$) would recycle an estimated 4.3 g m^{-2} of biomass (2.15 g m^{-2} of carbon) within the microbial mat at an average efficiency of 30% [43]. These first-order approximations are likely to be sensitive to inter-annual climate variability and changes to the ice shelf surface mass balance [46,47].

4.2. Effects of temperature

Ward Hunt Ice Shelf photosynthetic rates increased with temperature up to at least 20 °C, suggesting a growth optimum above 15 °C (i.e., psychrotrophic, sensu Morita, not psychrophilic), which is common for polar microbial mats [5]. The heterotrophic bacterial production did not respond coherently to temperature increases, suggesting that some members of the community were psychrophilic, while others were psychrotrophic with perhaps even some mesophilic organisms. The average Q_{10} value for photosynthesis was 1.88 (SE = 0.15). This value is close to the theoretical value of 2 for temperature dependent kinetic effects [48,49]. These values also compare with those found by Vincent et al. [40] (Q_{10} = 1.6–3.2), while a much higher degree of temperature responsiveness was found by Tang et al. [5] (Q_{10} = 4.85, but with large variability).

4.3. Effects of salinity

The effect of salinity on primary productivity suggests a broad growth optimum between 3 and 29 mS cm^{-1} for these ice-mat autrotrophs. Our results suggest that these microbial mats can not only tolerate higher salinities, but also prefer them to ambient conditions. Many microbial mats are found in saline [50,51] and hypersaline conditions [52,53]. This includes Antarctic ice shelf mats, where Hawes et al. [54] investigated the microbial mat response to gradual increases in salinity (from 5 to 160 mS cm^{-1}) and found no change in photosynthetic rate (relative to controls) up to 20 mS cm^{-1}. In contrast to the autotrophic community, the heterotrophic bacterial productivity did not respond favourably to increased salinity, suggesting that the bulk of this community was much more closely adapted to ambient conditions at the time of sampling. We suggest that this community may undergo a seasonal succession due to sharper growth optima relative to the more generalist phototrophs.

4.4. Effects of desiccation

Ward Hunt Ice Shelf microbial mats are not likely to dry out in situ, as they are relatively thin (1–2 cm), lie directly on the ice, and continuously receive moisture from the ice surface during the melt season. However, the effects of drying on mat organisms have implications for their dispersal from land to the ice shelf. In addition, the lowering of water activity associated with desiccation is analogous to the effects of freezing. Hawes et al. [55] found that microbial mat metabolic activity returns within minutes to hours after re-hydration. Mat-forming cyanobacteria are protected against freezing and dehydration by extrapolymeric substances (EPS) and water stress proteins contained within their sheaths [32,35,56]. These polysaccharide sheaths provide a physical barrier against the flow of water and may play a role in repelling bacterial and viral attack. If heterotrophic bacteria were located outside the cyanobacterial sheaths, they may not have benefited from intra-sheath moisture retained during the drying period, and would have been unduly affected by the desiccation of their immediate environment. A mid-season bacterial community specifically adapted to high water availability could also explain the different responses to desiccation between the autotrophic and heterotrophic bacterial communities.

4.5. Effects of light transition

Changes from snow-shaded to ambient light levels and the reverse did not affect the P_{max} of microbial mat photosynthesis. However, the photoinhibition parameter (β) was higher under low irradiances (at least by a factor of 10) in the light transition experiments and β was also higher in the low irradiance assay versus the high irradiance assay (Figs. 2(a) and (b)). This parameter shifted in concert with values of E_k and α, which is indicative of a reorganization of the photosynthetic apparatus to increased efficiency at lower irradiances, leaving the community prone to photoinhibition outside its acclimation window [57].

The relative stability of P_{max} across all treatments demonstrates that the mats can acclimate to light conditions associated with snow accumulation and ice-over, as well as with melting. Depending on the winter snowfall pattern and the following summer melt regime, we have observed that the microbial mats may remain buried under snow for one or possibly several summer seasons. The annual surface mass balance of the Ward Hunt Ice Shelf is positive when snowfall exceeds melting, and is negative when the opposite is true. As climate fluctuates over time scales of decades to centuries, the thickness of the ice shelf may change appreciably. After successive years of positive surface mass balance, microbial mats may reach a depth where they do not thaw or receive light in the summer. However, these microbial mats may be re-exposed and re-commence their metabolic activity after successive years of negative surface mass balance melts overlying ice and snow. Therefore, the present day ice shelf microbial mats are likely to be a heterogeneous community of variable age, composed of modern micro-organisms as well as ancient microbial mats that lived some time ago and have come

to the surface due to climatic shifts since the end of the Little Ice Age [58].

4.6. Pigments

Chlorophyll *a* levels from mats in high biomass areas of the Ward Hunt and Markham Ice Shelves were high relative to other microbial mats from many ponds and lakes throughout the polar regions, including meltwater ponds on the McMurdo Ice Shelf, Antarctica. One possible explanation is the cold temperatures on ice shelves preserve the chlorophyll molecules inside senescent cells for long periods. Low rates of heterotrophic bacterial production and small proportions of chlorophyllides and pheophytins support this low degradation hypothesis. McMurdo Ice Shelf microbial mats often lie atop relatively thick sediment, which likely warm to temperatures not experienced on northern ice shelves. The disparity between the McMurdo Ice Shelf and the northern ice shelves in this study may also be explained by sampling strategy (McMurdo sampling was randomized [59,60] unlike our targeting of the highest available biomass) and extraction methods [59,60]. Finally, there may be extra accumulation of chlorophyll *a* on the northern ice shelves due to recent climatic shifts that allowed buried microbial mats to re-emerge.

Carotenoids serve as photosynthetic accessory pigments and as cellular protection against reactive oxygen species [61]. They were found in abundance in northern ice shelf microbial mats, and in some cases, they exceeded the range of carotenoid concentration reported from Antarctica [62], and the Arctic [63] including those previously measured on Markham Ice Shelf [3]. However, the ratio of carotenoids to chlorophyll *a* was not as high as in Antarctica [62,64] and in nearby arctic mats [63], possibly reflecting the preservation and accumulation of large standing stocks of chlorophyll *a* on northern ice shelves.

Scytonemin is a cyanobacterial sheath pigment that is well-known to protect against UV-A radiation [23] and is found in very high concentrations in microbial mats containing Nostocales (up to 420 $\mu g\ cm^{-2}$, [62]). In the ice shelf mats, the concentrations were variable, and ranged up to a maximum of 262 $\mu g\ cm^{-2}$. We also observed high values of red scytonemin, indicating that scytonemin was reduced and accumulating on the ice shelf. The ratio of scytonemin to red scytonemin may be an indicator of reducing conditions for the site, as suggested for other environments [3,65]. The relative temporal stability of these sheath pigments supports the hypothesis that the Markham Ice Shelf site and Ward Hunt Site B are older and/or more reduced than Site A, as evidenced by the red scytonemin to chlorophyll *a* ratio and the scytonemin to red-scytonemin ratios (Table 2). However, this assumes a constant species composition and comparable pigment production rates across space and time. High proportions of red scytonemin may also be indicative of site-specific surface ablation history. If microbial mats were buried at sometime during the past millennium and were kept in reducing conditions, this pigment could re-emerge along with ancient microbial mat material, as discussed above, and could be a valuable paleoglaciological tool for discerning past climates on the ice shelf.

4.7. Mycosporine-like amino acids

Mycosporine-like amino acids are compounds that absorb in the UV-B and UV-A wavebands [31] and there is considerable evidence that they play a role in UV screening in a variety of organisms [66,67]. To date, OS-MAAs have been isolated from the sheaths of *Nostoc commune* [68] and this compound has been reported in related species (*Calothrix* sp. and cf. *Diplocolon* sp. [69]), but has not been previously reported from microbial mat consortia. However, the presence of this class of compounds in our sampling sites is to be expected since these ice shelf microbial mats have been found to contain a large proportion of *Nostoc* spp. [3]. OS-MAA concentrations in these microbial mats are almost two orders of magnitude lower than reported elsewhere (up to 2% of cellular dry weight [33]). However, ice shelf microbial mats appear to have very high values of OS-MAA when normalized to chlorophyll *a* relative to this other study (4.6 g OS-MAA (g Chl $a)^{-1}$ after 4.5 days of UV-B treatment, versus a control of 0.6 g OS-MAA (g Chl $a)^{-1}$[33]). This was a surprising result (especially for Site A, where the OS-MAA to total scytonemin ratio was $\sim$7 times higher than the other two sites, Table 2) since OS-MAA compounds are water-soluble and do not accumulate as readily as lipophilic scytonemin. High amounts of OS-MAAs at Site A could reflect a difference in community composition or the need for additional UV-B protection in these relatively thin mats.

4.8. Broadband pigment strategies

Our HPLC analysis indicates that arctic ice shelf microbial mats contain a broadband pigment assemblage that absorbs from the near UV-B to red PAR, and probably beyond given the pigment indication (okenone) of photosynthetic bacteria. These pigments can be classed as screening compounds (OS-MAAs, scytonemins), light harvesting and accessory pigments (chlorophylls, phycobiliproteins and certain carotenoids), and anti-oxidants (certain carotenoids and perhaps MAAs [70]). The presence of these pigments implies that these micro-organisms can spectrally modify their environment for photo-protection and photosynthetic efficiency. Furthermore, the presence of anti-oxidants confers an added mechanism for dealing with a combination of physiological stressors. The extracellular loca-

tion of OS-MAA and scytonemin greatly enhances the sunscreening factor for the cells over almost the entire naturally occurring UV waveband [69]. A broadband pigment strategy in the arctic ice shelf microbial mats is a means to control the spectral environment and allows the photosynthetic communities to tolerate the changing stresses of their cryo-habitat. This extremotrophic response is likely to be a strategy that also operates in other types of extreme environments. Other microbial inhabitants of the mat consortium, such as the heterotrophic bacteria and non-pigmented protists, may also benefit from the presence of pigments in their surroundings, although possibly not to the same degree as the organisms that produce these compounds.

5. Conclusion

Arctic ice shelf microbial mat consortia have relatively high primary productivity and low bacterial productivity, reflecting, in part, the relative proportion of autotrophs to heterotrophs. Consistent with our central hypothesis, the productivity experiments show that the ice shelf autotrophic community subsists in sub-optimal conditions, but can easily tolerate a wider range of environmental conditions including sudden changes in several key environmental variables in the ice shelf environment. Contrary to this hypothesis, however, the heterotrophic bacteria appeared to be adapted to the ice shelf microbial mat environment at the time of sampling and did not tolerate departures from these conditions as readily as the photosynthetic community. Considering that colonial cyanobacteria and algae in these mats are likely to have much longer generation times by comparison with heterotrophic bacteria, these autotrophic communities may therefore be more dependent upon tolerance rather than close acclimation to ambient conditions [71]. This would allow the autotrophic community to retain a large biomass, despite sub-optimal growth, providing that loss rates are small and that there was little competition by extremophilic species with adapted, faster rates of growth under in situ conditions [4]. In contrast, the shorter generation times in the heterotrophic bacterial community may allow successional shifts in community structure to be a strategy to deal with seasonal environmental change.

The broadband pigment assemblage, contained within the microbial mats enables the autotrophic community to cope with the combined effect of several environmental stressors, including the synergistic effects of low temperatures and high solar irradiances. The strategic use of these pigments may partly account for their extremotrophic physiological response to changes in environmental conditions. Heterotrophic bacteria appear to be less tolerant of variability and more adapted to the specific, extreme conditions at the time of sampling. These heterotrophic micro-organisms are therefore extremophilic, while the photosynthetic components of the mat consortium would be better classified as extremotrophs.

Acknowledgements

We thank the Natural Sciences and Engineering Research Council of Canada for funding support (graduate fellowship to D.R.M. and a Discovery Grant to W.F.V.), the Polar Continental Shelf Project (this is PCSP/EPCP manuscript 03304) and the Northern Scientific Training Program for financial and logistical support. Quttinirpaaq National Park provided assistance and the use of their facilities. Field assistance was provided by Katie Breen, Sébastien Roy and Jeffrey Kheraj, and laboratory assistance was provided by Marie-Josée Martineau. We thank two anonymous reviewers for their comments on the manuscript.

References

[1] Priscu, J.C. and Christner, B.C. (2004) Earth's icy biosphere In: Microbial Diversity and Bioprospecting (Bull, A., Ed.), pp. 130–145. American Society for Microbiology, Washington, DC.
[2] Vincent, W.F., Gibson, J.A., Pienitz, R., Villeneuve, V., Broady, P.A., Hamilton, P.B. and Howard-Williams, C. (2000) Ice shelf microbial ecosystems in the High Arctic and implications for life on snowball Earth. Naturwissenschaften 87, 137–141.
[3] Vincent, W.F., Mueller, D.R. and Bonilla, S. (2004) Ecosystems on ice: the microbial ecology of Markham Ice Shelf in the high Arctic. Cryobiology 48, 103–112.
[4] Vincent, W.F. (2000) Cyanobacterial dominance in the polar regions In: The Ecology of Cyanobacteria (Whitton, B.A. and Potts, M., Eds.), pp. 321–340. Kluwer Academic Press, The Netherlands.
[5] Tang, E.P.Y., Tremblay, R. and Vincent, W.F. (1997) Cyanobacteria dominance of polar freshwater ecosystems: are high-latitude mat-formers adapted to low temperature?. J. Phycol. 33, 171–181.
[6] Nadeau, T.L. and Castenholz, R.W. (2000) Characterization of psychrophilic oscillatorians (Cyanobacteria) from antarctic meltwater ponds. J. Phycol. 36, 914–923.
[7] Ehling-Schulz, M. and Scherer, S. (1999) UV protection in Cyanobacteria. Eur. J. Phycol. 34, 329–338.
[8] Cockell, C.S. and Knowland, J. (1999) Ultraviolet radiation screening compounds. Biol. Rev. Camb. Philos. Soc. 74, 311–345.
[9] Roos, J.C. and Vincent, W.F. (1998) Temperature dependence of UV radiation effects on Antarctic cyanobacteria. J. Phycol. 34, 118–125.
[10] Vincent, W.F., Mueller, D.R., Van Hove, P. and Howard-Willams, C. (2004) Glacial periods on early Earth and implications for the evolution of life In: Origins: Genesis, Evolution and Diversity of Life (Seckbach, J., Ed.), pp. 481–501. Kluwer Academic Publishers, Dortrecht.
[11] Jeffries, M.O. (2002) Ellesmere Island ice shelves and ice islands. In: Satellite Image Atlas of Glaciers of the World: Glaciers of North America (Williams, R.S. and Ferrigno, J.G., Eds.), pp. J147–J164. United States Geological Survey, Washington.

[12] Debenham, F. (1920) A new mode of transportation by ice: the raised marine muds of South Victoria Land. Q. J. Geol. Soc. 75, 51–76.
[13] Stal, L.J. (1995) Physiological ecology of cyanobacteria in microbial mats and other communities. New Phytologist 131, 1–32.
[14] Sakshaug, E., Bricaud, A., Dandonneau, Y., Falkowski, P.G., Kiefer, D.A., Legendre, L., Morel, A., Parslow, J. and Takahashi, M. (1997) Parameters of photosynthesis: definitions, theory and interpretation of results. J. Plankton Res. 19, 1637–1670.
[15] Platt, T., Geallegos, C. and Harrison, W.G. (1980) Photoinhibition of photosynthesis in natural assemblages of marine phytoplankton. J. Mar. Res 38, 687–701.
[16] Kirchman, D.L. (1993) Leucine incorporation as a measure of biomass production by heterotrophic bacteria In: Handbook of Methods in Aquatic Microbial Ecology (Kemp, P.F., Sherr, B.F., Sherr, E.B. and Cole, J.J., Eds.), pp. 509–512. Lewis Pub., Boca Raton.
[17] JGOFS, 1996. Protocols for Joint Global Ocean Flux Study Core Measurements, pp. 171–177, International Ocean Commission, Bergen, Norway.
[18] Strickland, J.D.H. and Parsons, T.R. (1972) Practicle Seawater Analysis, 2nd edn. Fisheries Research Board, Canada, Ottawa.
[19] Villeneuve, V., 2000. Algues benthiques du haut Arctique canadien: microhabitat et évaluation des facteurs de contrôle chimiques, M.Sc. Thesis, Department of Biology, Laval University, Quebec, QC.
[20] Zapata, M., Rodriguez, F. and Garrido, J.L. (2000) Separation of chlorophylls and carotenoids from marine phytoplankton: a new HPLC method using a reversed phase C8 column and pyridine containing mobile phases. Mar. Ecol. Prog. Ser. 195, 29–45.
[21] Hertzberg, S. and Liaan-Jensen, S. (1969) The structure of Oscillaxanthin. Phytochemistry 8, 1281–1292.
[22] Jeffrey, S.W., Mantoura, R.F.C. and Wright, S.W. (1997) Phytoplankton Pigments in Oceanography. SCOR UNESCO, Paris.
[23] Garcia-Pichel, F., Sherry, N.D. and Castenholz, R.W. (1992) Evidence for an ultraviolet sunscreen role of the extracellular pigment scytonemin in the terrestrial cyanobacterium *Chlorogloeopsis* sp. Photochem. Photobiol. 56, 17–23.
[24] Shick, J.M., Romaine-Lioud, S., Ferrier-Pagès, C. and Gattuso, J.P. (1999) Ultraviolet-B radiation stimulates shikimate pathway-dependent accumulation of mycosporine-like amino acids in the coral *Stylophora pistillata* despite decreases in its population of symbiotic dinoflagellates. Limnol. Oceanogr. 44, 1667–1682.
[25] Sommaruga, R. and Garcia-Pichel, F. (1999) UV-absorbing mycosporine-like compounds in planktonic and benthic organisms from a high-mountain lake. Archiv. Hydrobiol. 144, 255–269.
[26] Böhm, G.A., Pfeiderer, W., Böger, P. and Scherer, S. (1995) Structure of a novel oligosaccharide-mycosporine-amino acid ultraviolet A/B sunscreen pigment from the terrestrial cyanobacterium *Nostoc commune*. J. Biol. Chem. 270, 8536–8539.
[27] Schülter, L., Garde, K. and Kaas, H. (2004) Detection of the toxic cyanobacteria *Nodularia spumigena* by means of a 4-keto-myxoxanthophyll-like pigment in the Baltic Sea. Mar. Ecol. Prog. Ser. 275, 69–78.
[28] Francis, G.W., Hertzberg, S., Andersen, K. and Liaan-Jensen, S. (1970) New carotenoid glycosides from *Oscillatoria limosa*. Phytochemistry 9, 629–635.
[29] Goodwin, T.W. (1980) The Biochemistry of the Carotenoids, 2nd edn. Chapman and Hall, London New York.
[30] Fujii, R., Chen, C.-H., Mizoguchi, T. and Koyama, Y. (1998) ^{1}H NMR, electronic-absorption and resonance-Raman spectra of isomeric okenone as compared with those of isomeric β-carotene, canathaxanthin, β-apo-8′-carotenal and spheroidene. Spectrochim. Acta A Mol. Biomol. Spectrosc. 54, 727–743.
[31] Karentz, D., McEuen, F.S., Land, M.C. and Dunlap, W.C. (1991) Survey of mycosporine-like amino acid compounds in Antarctic marine organisms: potential protection from ultraviolet exposure. Marine Biol. 108, 157–166.
[32] Hill, D.R., Peat, A. and Potts, M. (1994) Biochemistry and structure of the glycan secreted by desiccation-tolerant *Nostoc commune* (Cyanobacteria). Protoplasma 182, 126–148.
[33] Ehling-Schulz, M., Bilger, W. and Scherer, S. (1997) UV-B-induced synthesis of photoprotective pigments and extracellular polysaccharides in the terrestrial cyanobacterium *Nostoc commune*. J. Bacteriol. 179, 1940–1945.
[34] Ito, S. and Hirata, Y. (1977) Isolation and structure of a mycosporine from the zoanthid. Tetrahed. Lett. 18, 2429–2430.
[35] Hill, D.R., Hladun, S.L., Scherer, S. and Potts, M. (1994) Water stress proteins of *Nostoc commune* (Cyanobacteria) are secreted with UV-A/B-absorbing pigments and associate with 1,4-β-D-xylanxylanohydrolase activity. J. Biol. Chem. 269, 7726–7734.
[36] Howard-Williams, C., Vincent, C.L., Broady, P.A. and Vincent, W.F. (1986) Antarctic stream ecosystems: variability in environmental properties and algal community structure. Int. Rev. ges. Hydrobiol. 71, 511–544.
[37] Howard-Williams, C. and Vincent, W.F. (1989) Microbial communities in southern Victoria Land streams (Antarctica). 1. Photosynthesis. Hydrobiologia 172, 27–38.
[38] Vincent, W.F., Castenholz, R.W., Downes, M.T. and Howard-Williams, C. (1993) Antarctic cyanobacteria: light, nutrients, and photosynthesis in the microbial mat environment. J. Phycol. 29, 745–755.
[39] Hawes, I. and Howard-Williams, C. (1998) Primary production processes in streams of the McMurdo Dry Valleys, Antarctica In: Ecosystem Dynamics in a Polar Desert: The McMurdo Dry Valleys, Antarctica (Priscu, J.C., Ed.), pp. 129–140. American Geophysical Union, Washington.
[40] Vincent, W.F. and Howard-Williams, C. (1989) Microbial communities in southern Victoria Land streams (Antarctica). 2. The effects of low temperature. Hydrobiologia 172, 39–49.
[41] Tuominen, L. (1995) Comparison of leucine uptake methods and a thymidine incorporation method for measuring bacterial activity in sediment. J. Microbiol. Meth. 24, 125–134.
[42] Bell, R.T. (1993) Estimating production of heterotrophic bacterioplankton via incorporation of tritiated thymidine In: Handbook of Methods in Aquatic Microbial Ecology (Kemp, P.F., Sherr, B.F., Sherr, E.B. and Cole, J.J., Eds.), pp. 495–504. Lewis Publication, Boca Raton.
[43] Fischer, H. and Pusch, M. (1999) Use of the [^{14}C]leucine incorporation technique to measure bacterial production in river sediments and the epiphyton. Appl. Environ. Microbiol. 65, 4411–4418.
[44] Kirchman, D.L. (1993) Estimating conversion factors for the thymidine and leucine methods for measuring bacterial production In: Handbook of Methods in Aquatic Microbial Ecology (Kemp, P.F., Sherr, B.F., Sherr, E.B. and Cole, J.J., Eds.), pp. 513–517. Lewis Publication, Boca Raton.
[45] Moorhead, D.L., Davis, W.S. and Wharton, R.A. (1997) Carbon dynamics of aquatic microbial mats in the Antarctic dry valleys: a modelling synthesis In: Ecosystem Processes in Antarctic ice-free Landscapes (Lyons, W.B., Howard-Williams, C. and Hawes, I., Eds.), pp. 181–196. A.A. Balkema, Rotterdam, Netherlands.
[46] Serson, H.V. (1979) Mass balance of the Ward Hunt Ice Rise and Ice Shelf: an 18-year record. Defence Establishment Pacific, Victoria, Victoria, BC, pp. 14.
[47] Lister, H. (1962) Heat and mass balance at the surface of the Ward Hunt Ice Shelf, 1960. Arctic Institute of North America, Washington, DC, pp. 54.
[48] Davison, I. (1990) Environmental effects on algal photosynthesis: temperature. J. Phycol. 27, 2–8.

[49] Falkowski, P.G. and Raven, J.A. (1997) Aquatic Photosynthesis. Blackwell Science, Malden, Mass.
[50] Yallop, M.L., Dewinder, B., Paterson, D.M. and Stal, L.J. (1994) Comparative structure, primary production and biogenic stabilization of cohesive and noncohesive marine-sediments inhabited by microphytobenthos. Estuar. Coast. Shelf Sci. 39, 565–582.
[51] Stal, L.J. (1994) Microbial mats in coastal environment In: Microbial mats (Stal, L.J. and Caumette, P., Eds.), pp. 21–32. Springer-Verlag, Berlin.
[52] Sorensen, K., Canfield, D. and Oren, A. (2004) Salinity responses of benthic microbial communities in a solar saltern (Eilat, Israel). Appl. Environ. Microbiol. 70, 1608–1616.
[53] Wieland, A. and Kuhl, M. (2000) Irradiance and temperature regulation of oxygenic photosynthesis and O_2 consumption in a hypersaline cyanobacterial mat (Solar Lake, Egypt). Marine Biol. 137, 71–85.
[54] Hawes, I., Smith, R., Howard-Williams, C. and Schwarz, A.M. (1999) Environmental conditions during freezing, and response of microbial mats in ponds of the McMurdo Ice Shelf. Antarctica. Ant. Sci. 11, 198–208.
[55] Hawes, I., Howard-Williams, C. and Vincent, W.F. (1992) Desiccation and recovery of cyanobacterial mats. Polar Biol. 12, 587–594.
[56] Decho, A.W. (1994) Exopolymers in microbial mats: Assessing their adaptive role In: Microbial Mats (Stal, L.J. and Caumette, P., Eds.), pp. 215–219. Springer-Verlag, Berlin.
[57] Behrenfeld, M.J., Prasil, O., Babin, M. and Bruyant, F. (2004) In search of a physiological basis for covariations in light-limited and light-saturated photosynthesis. J. Phycol. 40, 4–25.
[58] Crary, A.P., Kulp, J.L. and Marshall, E.W. (1955) Evidences of climatic change from ice island studies. Science 122, 1171–1173.
[59] Howard-Williams, C., Pridmore, R.D., Downes, M.T. and Vincent, W.F. (1989) Microbial biomass, photosynthesis and chlorophyll *a* related pigments in the ponds of the McMurdo Ice Shelf. Antarctica. Ant. Sci. 1, 125–131.
[60] Howard-Williams, C., Pridmore, R.D., Broady, P.A. and Vincent, W.F. (1990) Environmental and biological variability in the McMurdo Ice Shelf ecosystem In: Antarctic Ecosystems: Ecological Change and Conservation (Kerry, K.R. and Hempel, G., Eds.), pp. 23–31. Springer-Verlag, Berlin.
[61] Hirschberg, J. and Chamovitz, D. (1994) Carotenoids in cyanobacteria In: The Molecular Biology of Cyanobacteria (Bryant, D.A., Ed.), pp. 559–579. Kluwer Academic Publishers, Dordrecht.
[62] Vincent, W.F., Downes, M.T., Castenholz, R.W. and Howard-Williams, C. (1993) Community structure and pigment organisation of cyanobacteria-dominated microbial mats in Antarctica. Eur. J. Phycol. 28, 213–221.
[63] Villeneuve, V., Vincent, W.F., and Komárek, J., 2001. Community structure and microhabitat characteristics of cyanobacterial mats in an extreme high Arctic environment: Ward Hunt Lake, Vol. 123, Nova Hedwigia, Beiheft, pp. 199–224.
[64] Sabbe, K., Hodgson, D., Verleyen, E., Taton, A., Wilmotte, A., Vanhoutte, K. and Vyverman, W. (2004) Salinity, depth and the structure and composition of microbial mats in continental Antarctic lakes. Freshwater Biol. 49, 296–319.
[65] Garcia-Pichel, F. and Castenholz, R.W. (1991) Characterization and biological implications of scytonemin, a cyanobacterial sheath pigment. J. Phycol. 27, 395–409.
[66] Neale, P.J., Banaszak, A.T. and Jarriel, C.R. (1998) Ultraviolet sunscreens in *Gymnodinium sanguineum* (Dinophyceae): mycosporine-like amino acids protect against inhibition of photosynthesis. J. Phycol. 34, 928–938.
[67] Garcia-Pichel, F. and Castenholz, R. (1993) Evidence regarding the UV sunscreen role of a mycosporine-like compound in the cyanobacterium *Gloeocapsa* sp. Appl. Environ. Microbiol. 59, 170–176.
[68] Scherer, S., Chen, T.W. and Böger, P. (1988) A new UV-A/B protecting pigment in the terrestrial cyanobacterium *Nostoc commune*. Plant Physiol. 88, 1055–1057.
[69] Garcia-Pichel, F. and Castenholz, R. (1993) Occurrence of UV-absorbing mycosporine-like compounds among cyanobacterial isolates and an estimate of their screening ability. Appl. Environ. Microbiol. 59, 163–169.
[70] Dunlap, W.C. and Yamamoto, Y. (1995) Small-molecule antioxidants in marine organisms: antioxidant activity of mycosporine-glycine. Comp. Biochem. Physiol. B Biochem. Mol. Biol. 112B, 105–114.
[71] Vincent, W.F. and Quesada, A. (1997) Microbial niches in the polar environment and the escape from UV radiation in non-marine habitats In: Antarctic Communities: Species, Structure and Survival (Battaglia, B., Valencia, J. and Walton, D., Eds.), pp. 388–395. Cambridge University Press, Cambridge.